

1

Mid-ocean ridge eruptions as a climate valve

2

3

Maya Tolstoy

4

Lamont-Doherty Earth Observatory of Columbia University, 61 Route 9W,

5

Palisades, NY 10864-8000, U.S.A.

6 [1] Seafloor eruption rates, and mantle melting fueling eruptions, may be influenced by
7 sea-level and crustal loading cycles at scales from fortnightly to 100 kyr. Recent mid-
8 ocean ridge eruptions occur primarily during neap tides and the first 6 months of the year,
9 suggesting sensitivity to minor changes in tidal forcing and orbital eccentricity. An ~100
10 kyr periodicity in fast-spreading seafloor bathymetry, and relatively low present-day
11 eruption rates, at a time of high sea-level and decreasing orbital eccentricity suggest a
12 longer term sensitivity to sea-level and orbital variations associated with Milankovitch
13 cycles. Seafloor spreading is considered a small but steady contributor of CO₂ to climate
14 cycles on the 100 kyr time scale, however this assumes a consistent short-term eruption
15 rate. Pulsing of seafloor volcanic activity may feed back into climate cycles, possibly
16 contributing to glacial/inter-glacial cycles, the abrupt end of ice ages, and dominance of
17 the 100 kyr cycle.

18

19 1. Introduction

20 [2] The driving forces behind ice age cycles are hotly debated. In particular, the
21 abrupt end of ice ages and dominance of the 100 kyr signal in climate cycles are not well
22 understood [e.g. Shackleton, 2000; EPICA community members, 2004]. Orbital
23 eccentricity, which ties closely to the 100 kyr signal, is a relatively small forcing in terms
24 of insolation, and thus its association with the largest peaks in CO₂ is unexpected.
25 Seafloor spreading is generally viewed as a steady-state process on the 100 kyr time
26 scale. While some episodicity has been noted in seafloor bathymetry [e.g. Vogt et al.,
27 1969; Kappel & Ryan, 1986], only long-term variations in spreading rate having been
28 proposed to influence atmospheric CO₂ over the last 100 million years [Berner et al.,

29 1983; Miller et al., 2005]. Changes in hydrothermal output due to plate reorganization
30 have also been proposed to cause significant flux changes in CO₂ on the 10's of millions
31 of years time-scale [Owen & Rea, 1985], however major plate reorganizations are rare.

32 [3] Seafloor eruptions contribute to ocean CO₂ fluxes without the global cooling
33 effect associated with terrestrial eruptions due to volcanic particles injected into the
34 atmosphere [e.g. Robock, 2000]. However, until recently very little was known about
35 mid-ocean ridge eruptions because most occur far from land, at seismicity levels below
36 the detection capabilities of global seismic networks. Recent advances in seafloor
37 hydroacoustic monitoring have allowed the timing and character of seafloor eruptions to
38 be studied, in particular at intermediate and fast spreading ridges, beginning in 1993 and
39 1996 respectively [Fox et al., 1993; 2001].

40

41 2. Timing of Mid-Ocean Ridge Volcanic Activity

42 [4] Microearthquakes at mid-ocean ridges, which are sensitive to tidal forcing, occur
43 preferentially during times of maximum extensional stresses [Wilcock, 2001; Tolstoy et
44 al., 2002; Stroup et al., 2007]. Terrestrial volcanism has also been shown in some
45 locations to be sensitive to tidal periodicities [e.g. Johnston & Mauk, 1972], seasonal
46 loading and unloading [e.g. Mason et al., 2004], glacial loading, unloading [e.g. Jull and
47 McKenzie, 1996] and rate of unloading [e.g. Jellinek et al., 2004], as well as rate of
48 climatically driven sea-level change [McGuire et al., 1997]. However, timing of volcanic
49 activity with respect to tidal forcing at mid-ocean ridges has not previously been studied.
50 To date, nine mid-ocean ridge eruptions/diking events have been well documented in
51 terms of their timing, seismic character, and seafloor confirmation of likely magmatic

52 activity [Fox et al., 1995; Fox & Dziak, 1998; Dziak & Fox, 1999; Tolstoy et al., 1999;
53 2001; 2006; Bohnenstiehl et al., 2004; Dziak et al., 2004; 2012]. Figure 1 shows that
54 eight out of nine of these best-documented mid-ocean ridge magmatic events occurred
55 during lows in the fortnightly tidal modulations (neap tides). A Schuster test (Emter,
56 1997) shows statistically significant non-random distribution with respect to the
57 fortnightly modulations of the tides (99%). This suggests that seafloor eruptions are
58 particularly sensitive to prolonged tidal unloading and implies a system response time
59 [Jupp et al., 2004] that is generally longer than the diurnal and semi-diurnal tidal
60 fluctuations (Figure 2).

61 [5] An annual bias in eruption times is also evident (Figure 1) with all nine of these
62 events occurring preferentially during the period of ‘unloading’ in the annual solid-earth
63 tides, that is between the time of closest approach to the sun (early January) and the
64 furthest point from the sun (early July), during which the influence of the sun on the tides
65 is gradually decreasing. A further eruption can be added to this list where precise timing
66 is not known, but can be confidently placed in the March-April time frame based on
67 submersible observations (Haymon et al., 1993), making the ten observations statistically
68 significant (Schuster Test, 96%). This may reflect a long-wavelength sensitivity of
69 melting at depth, melt transport and/or dike formation, due to lithospheric/asthenospheric
70 extension and unloading. The thin seafloor lithosphere in this extensional environment
71 would make seafloor volcanism much more sensitive to deformation due to eccentricity
72 compared to terrestrial settings. The apparent sensitivity of mid-ocean ridge magmatism
73 to this relatively minor yearly orbital perturbation implies that it may also be sensitive to
74 long-term orbital perturbations, thus linking seafloor volcanism to the Milankovitch

75 cycles observed so strongly in climate data. The eccentricity of Earth's orbit, which tracks
76 the largest ~100 kyr climate cycle [Hayes et al., 1976], is the orbital variation that should
77 produce the largest direct forcing on seafloor volcanism, since maximum eccentricity
78 (0.06) corresponds to an ~18 million km difference in the point of closest and furthest
79 approach to the sun, compared with 100-1000's of km differences in solar proximity
80 caused by variations in orbital precession and obliquity. Increases in orbital eccentricity
81 should have the effect of increasing this apparent annual seafloor volcanic forcing.

82 [6] Variations in sea-level associated with climatic cycles, and in particular ice ages,
83 may similarly impact the rate of melting and volcanism throughout the world's oceans
84 (Lund & Asimow, 2011). Sea-level fluctuations due to ice age cycles are on the order of
85 100 m on the 5,000 - 100,000 year time scale [e.g. Miller et al., 2005]. The decrease in
86 sea-level (unloading), associated with an ice age would lead to an increase in oceanic
87 mantle melting and an increase in seafloor volcanism. Similarly, an increase in sea-level
88 (loading) would have the opposite effect, suppressing melting in the mantle for some
89 time. The deformation due to sea-level changes needs to be considered in combination
90 with deformation associated with variations in orbital eccentricity as well as considering
91 system response times.

92 [7] The time scale for the response of the seafloor and mantle is dependent on the rate
93 of loading or unloading, the lithospheric thickness and asthenospheric viscosity. How
94 fluctuations in melting feed back into dike initiation and eruption rates is also dependent
95 on unloading rate. The mechanism of melt transport through the mantle is not well
96 understood [e.g. Phipps Morgan & Holtzman, 2005] and thus understanding the impact of
97 varied lithospheric and asthenospheric deformation on melt transport is difficult.

98 Furthermore, current literature disagrees on the rate of melt transport in the mantle by as
99 much as three orders of magnitude [Elliott, 2005]. Therefore it is difficult to accurately
100 model the quantitative impact of sea-level changes combined with changes in orbital
101 eccentricity both in terms of volume of melt, and in terms of system lag time. However,
102 simple calculations based on upwelling rates and isostatic responses suggest that system
103 lag time might be on the order of 100's to 1000's of years, and observations from
104 terrestrial systems suggest lag times of ~1-11 kyr [Jull & MacKenzie, 1996; Jellinek et
105 al., 2004]. Such times are broadly consistent with modeling of sea-level influence alone
106 [Lund & Asimow, 2011], however this modeling suggests changes in magma flux would
107 be least significant at fast-spreading ridges. The absence of strong peaks associated
108 shorter period sea-level changes suggests magma flux at the SEPR may also be
109 responding directly to 100 kyr orbital eccentricity changes.

110 [8] Since we are currently in a period of relatively high sea-level and lower orbital
111 eccentricity (0.0167), a model proposing sensitivity to these forcings would predict that
112 current rates of seafloor volcanism would be lower than expected from simple spreading
113 rate calculations. Present day eruption data supports this hypothesis. Hydroacoustic
114 monitoring at the East Pacific Rise [Fox et al., 1995], northern Mid-Atlantic Ridge
115 [Smith et al., 2002], and Juan de Fuca Ridge [Fox et al., 1994] all show significantly
116 fewer eruptions than would be predicted based on spreading rates and the assumption of 1
117 m of opening (dike width) per eruption (Supporting Text S1).

118

119 3. Bathymetric evidence for pulsing of seafloor volcanism

120 [9] Seafloor spreading would continue regardless of the stage of the climatic or
121 orbital cycle. However, the sensitivity of melting and eruptions to loading and unloading
122 from sea-level and orbital forcings would predict fluctuations in the amount of seafloor
123 volcanism associated with this sustained spreading, particularly at the 100 kyr
124 periodicity. Seafloor topography considered in terms of spreading rate may provide clues
125 to fluctuations in magmatism over 10's of thousands of years. The Southern East Pacific
126 Rise (SEPR) provides a site where faulting is least dominant, and magmatism is most
127 prevalent. A period dominated by magmatism may have thicker crust, or shallower
128 bathymetry, due to a thicker layer of surface extrusive volcanics (Layer 2A), and/or less
129 thinning from faulting. A period of decreased eruptions, with fewer dike events, or
130 fewer dikes that reached the surface, may have a thinner layer of extrusive volcanics,
131 and/or more thinning due to faulting, resulting in deeper bathymetry. While a lag is
132 predicted between forcings and eruptions, during voluminous eruptions it is common for
133 lava to flow away from the axis 100's of m's to as much as 2 km, meaning that lava is
134 built up on seafloor that is 1000's to 10,000's of years older than the eruption itself, thus
135 perhaps counteracting the system lag in terms of seafloor appearance.

136 [10] At 17°S the SEPR is spreading at a full rate of ~14.7 cm/yr [Scheirer et al.,
137 1996], and high-resolution bathymetric maps extend 100's of km off-axis. Figure 3A
138 compares bathymetry for ~775 kyr of spreading on the western side of the SEPR at 17°S
139 (Supporting Figure S1), with a ~800 kyr CO₂ time series from Antarctic ice-cores [Lüthi
140 et al, 2008, and references therein], (which broadly follows sea-level at longer time
141 periods), as well as orbital eccentricity [Varadi et al., 2003], which ties closely to the
142 ~100 kyr periodicity in Milankovitch cycles. A visual comparison indicates correlation

143 between periods of low CO₂, low orbital eccentricity and periods of apparent decreased
144 magmatism, as well as periods of abruptly increasing CO₂, and abruptly increasing
145 magmatism, and high orbital eccentricity. An examination of the spectral energy of these
146 data supports this interpretation, with peaks at a wavelength near 100 kyr for both the
147 bathymetric, CO₂ and eccentricity data (Figure 3B). Normalized overlays of the
148 bathymetry and CO₂ (Supporting Figure S2) and bathymetry and eccentricity
149 (Supporting Figure S3) further illustrate that the 100 kyr cycles appear to be broadly in
150 phase.

151

152 4. Discussion and Conclusions

153 [11] There are several ways in which seafloor volcanism can contribute to global
154 climate change. The first is the direct emission of CO₂ into the ocean that will eventually
155 contribute to atmospheric levels through venting at upwelling sites. In addition to
156 immediate release of greenhouse gases from seafloor eruptions, the subsequent increased
157 high and low temperature hydrothermal venting may impact the CO₂ output. However,
158 whether hydrothermal venting is a net source or sink of CO₂ is still unclear (e.g. Lang et
159 al., 2006), due to paucity of measurements.

160 [12] Overall, the average annual contribution of CO₂ from seafloor spreading is
161 generally considered to be small though not insignificant ($\sim 2 \times 10^{12}$ mol/yr) [e.g. Resing
162 et al., 2004] with respect to the global carbon cycle. However, this assumes a model of
163 near continuous release, whereas a model of frequent pulses of activity followed by
164 quiescent periods might result in more significant pulses of CO₂ into the global carbon

165 system. Approximately 2 km of glacial unloading in Iceland resulted in volcanism rates
166 20-30 times higher than today [Jull & McKenzie, 1996].

167 [13] Changes in sea-level of ~100 m and changes in the forcing from orbital
168 eccentricity applied to the relatively thin oceanic lithosphere, across a broad area may
169 result in a smaller but nevertheless significant pulsing of seafloor volcanism. The large
170 spatial extent of mid-ocean ridges means that even a small increase in the melting and
171 volcanism rate may have significant consequences for the global carbon budget. A CO₂
172 production rate of $\sim 2 \times 10^{12}$ mole/yr is ~ 0.088 gT/yr or ~ 0.041 ppmv of CO₂. For
173 instance, an increase of only 50% in the eruption rate over the ~ 5 kyr typical for abrupt
174 ends to ice-ages would thus theoretically result in an ~ 100 ppmv rise in CO₂. However,
175 the transport of CO₂ from the seafloor to the atmosphere is physically and geochemically
176 complex and likely only a fraction reaches the atmosphere (Huybers & Langmuir, 2009).
177 The contribution of off-axis volcanism, submarine back-arc volcanism, and island arc
178 volcanism, which would also be influenced by loading and unloading, may be an
179 additional factor.

180 [14] This pulsing would provide a mechanism for seafloor volcanism to act as a
181 negative climate feedback with respect to glaciation, but potentially a direct contributor
182 to climate change through geophysical responses to changes in orbital eccentricity.
183 Release of greenhouse gases would increase during periods of extreme glaciation and/or
184 high orbital eccentricity, and decrease following periods of glacial melting and/or low
185 orbital eccentricity. The glacial dependence is consistent with observations that ice-sheet
186 volume lags CO₂ and temperature variations in 100 kyr ice age cycles [Shackleton,
187 2000]. While loading and unloading due to sea-level change is likely to influence melting

188 on the 1000's of years time scale, the timing of variations in eruption rates may also be
189 influenced by orbital eccentricity as well as the variability in the rate of change of sea-
190 level. Fluctuations in eruption rates may thus be a complex interplay of the forcings
191 associated with sea-level, rate of change of sea-level, and orbital eccentricity, likely
192 leading to short-term fluctuations on the 1000's of years time scale with a longer term
193 ~100 kyr cycle superimposed.

194 [15] Estimates of the effect of seafloor spreading on the global carbon cycle and
195 greenhouse gases are not well constrained, but are based largely on calculations that
196 assume steady-state input from steady-state spreading. Seafloor bathymetry and present
197 day sensitivity to tidal and orbital forcing indicate that this steady-state assumption may
198 not be accurate on the time scale of cycles observed in climate variability (1000's to
199 ~100,000 years). Instead, while seafloor spreading may be relatively constant on average,
200 seafloor volcanism could be viewed as a highly variable process that may increase and
201 decrease with climatic and orbital forcing, acting as a climatic valve that causes the flow
202 of greenhouse gases to fluctuate.

203

204 5. Acknowledgements

205 [14] Data used here are available through the Marine Geoscience Data System
206 (<http://www.marine-geo.org/portals/gmrt/>) and in references cited. This work was
207 supported by NSF under grants OCE-0327283 , OCE-0732569, and OCE-0961594, as
208 well as LDEO. I thank R.F. Anderson, W.S. Broecker, W.R. Buck, T.J. Crone, A.M.
209 Jellinek, B. Liepert, W.R. McGillis, R. Newton and D. Peteet for many useful discussions
210 and comments on the manuscript. I thank E.T. Baker for an early particularly constructive

211 and thoughtful review. I also thank P. Vogt and P. Huyber for reviews that improved the
212 manuscript.

213

214 **References**

215 Berner, R.A., A.C. Lasaga, and R.M. Garrels (1983), The carbonate-silicate geochemical
216 cycle and its effect on atmospheric carbon dioxide over the past 100 million years,
217 *Amer. J. Sci.*, 283, 641-683.

218 Bohnenstiehl, D.R., R.P. Dziak, M. Tolstoy, C. Fox, and M. Fowler (2004), Temporal
219 and Spatial History of the 1999-2000 Endeavour Seismic Series, Juan de Fuca Ridge,
220 *Geochem. Geophys. Geosys.* 5, doi:10.1029/2004GC000735.

221 Dziak, R.P., and C.G. Fox (1999), The January 1998 earthquake swarm at axial volcano,
222 Juan de Fuca Ridge: Hydroacoustic evidence of seafloor volcanic activity, *Geophys.*
223 *Res. Lett.*, 26, 3429-3432.

224 Dziak, R.P., D. Smith, D. Bohnenstiehl, C. Fox, D. Desbruyeres, H. Matsumoto, M.
225 Tolstoy, and D. Fornari (2004), Evidence of a recent magma dike intrusion at the
226 slow-spreading Lucky Strike segment, Mid-Atlantic Ridge, *J. Geophys. Res.*, 109,
227 doi:10.1029/2004JB003141.

228 Dziak, R.P., J.H. Haxel, D.R. Bohnenstiehl, W.W. Chadwick, S.L. Nooner, M.J. Fowler,
229 H. Matsumoto, and D.A. Butterfied (2012), Seismic precursors and magma ascent
230 before the April 2011 eruption at Axial Seamount, *Nature Geoscience*, 5, doi:
231 10.1038/ngeo1490.

232 Elliott, T. (2005), Earth science – Unleaded high-performance, *Nature*, 437, doi:
233 10.1038/437485a.

234 EPICA community members (2004), Eight glacial cycles from an Antarctic ice core,
235 Nature, 429, 623-628.

236 Fox, C.G., R.P. Dziak, H. Matsumoto, and A.E. Schreiner (1993), Potential for
237 monitoring low-level seismicity on the Juan de Fuca Ridge using military hydrophone
238 arrays, Mar. Tech. Soc., 27, 22-29.

239 Fox, C.G., W.E. Radford, R.P. Dziak, T.K. Lau, H. Matsumoto, A.E. Schreiner (1995),
240 Acoustic detection of a sea-floor spreading episode on the Juan-de-Fuca Ridge using
241 military hydrophone arrays, Geophys. Res. Lett., 22, 131-134.

242 Fox, C.G., and R.P. Dziak (1998), Hydroacoustic detection of volcanic activity on the
243 Gorda Ridge, February-March 1996, Deep-Sea Res. II, 12, 2513-2530.

244 Fox, C.G., H. Matsumoto, and T.-K. Lau (2001), A. Monitoring Pacific Ocean seismicity
245 from an autonomous hydrophone array, J. Geophys. Res., 106, 4183-4206.

246 Haymon, R.M., D.J. Fornari, K.L. Von Damm, M.D. Lilley, M.R. Perfit, J.M. Edmond,
247 W.C. Shanks III, R.A. Lutz, J.B. Grebmeier, S. Carbotte, D. Wright, E. McLaughlin,
248 E. Smith, N. Beedle, and E. Olson (1993), Volcanic eruption of the mid-ocean ridge
249 along the East Pacific Rise crest at 9°45-52'N: Direct submersible observations of
250 seafloor phenomena associated with an eruption event in April, 1991, Earth Planet.
251 Sci. Lett., 11, 85-101.

252 Hays, J.D., J. Imbrie, and N.J. Shackleton (1976), Variations in the Earth's Orbit:
253 Pacemaker of the Ice Ages, Science, 194, 1121-1132.

254 Huybers, P., C. Langmuir (2009), Feedback between deglaciation, volcanism, and
255 atmospheric CO₂, Earth Planet. Sci. Lett., 286, 479-491.

256 Jellinek, A.M., M. Manga, and M.O. Saar (2004), Did melting glaciers cause volcanic
257 eruptions in eastern California? Probing the mechanics of dike formation, *J. Geophys.*
258 *Res.*, 109, doi:10.1029/2004JB002978.

259 Johnston, M. J., and F.J. Mauk (1972), Earth Tides and the Triggering of Eruptions from
260 Mt Stromboli, Italy, *Nature*, 239, 266-267.

261 Jull, M., and D. McKenzie (1996), The effect of deglaciation on mantle melting beneath
262 Iceland, *J. Geophys. Res.*, 101, 21815-21828.

263 Jupp, T.E., D.M. Pyle, B.G. Mason, and W.B. Dade (2004), A statistical model for the
264 timing of earthquakes and volcanic eruptions influenced by periodic processes, *J.*
265 *Geophys. Res.*, 109, doi:10.1029/2003JB002584.

266 Kappel, E.S., and W.B.F. Ryan (1986), Volcanic Episodicity and a Non-Steady State Rift
267 Valley Along Northeast Pacific Spreading Centers, *J. Geophys. Res.*, 91, pp 13,925-
268 13,940.

269 Lüthi, D., M. Le Floch, B. Bereiter, T. Blunier, J.-M. Barnola, U. Siegenthaler, D.
270 Raynaud, J. Jouzel, H. Fischer, K. Kawamura, and T.F. Stocker (2008), High-
271 resolution carbon dioxide concentration record 650,000-800,000 years before present,
272 *Nature*, 453, 379-382.

273 Lund, D.C., and P.D. Asimow (2011), Does sea level influence mid-ocean ridge
274 magmatism on Milankovitch timescales? *Geochem. Geophys. Geosys.* 12,
275 doi:10.1029/2011GC003693.

276 Mason, B.G., D.M. Pyle, W.B. Dade, and T. Jupp (2004), Seasonality of volcanic
277 eruptions. *J. Geophys. Res.* 109, doi:10.1029/2002JB002293.

278 Matsumoto, K.T., T. Takanezawa, and M. Ooe (2000), Ocean tide models developed by
279 assimilating TOPEX/POSEIDON altimeter data in hydrodynamical model: A global
280 model and a regional model around Japan, *J. Oceanogr.*, 56, 567-581.

281 McGuire, W.J., R.J. Howarth, C.R. Firth, A.R. Solow, A.D. Pullen, S.J. Saunders, I.S.
282 Stewart, and C. Vita-Finzi (1997), Correlation between rate of sea-level change and
283 eney of explosive volcanism in the Mediterranean, *Nature*, 389, 473-476.

284 Miller, K.G., M.A. Kominz, J.V. Browning, J.D. Wright, G.S. Mountain, M.E. Katz, P.J.
285 Sugarman, B.S. Cramer, N. Christie-Blick, and S.F. Pekar (2005), The Phanerozoic
286 Record of Global Sea-Level Change, *Science*, 310, 1293-1298.

287 Owen, R.M., and D.K. Rea (1985), Seafloor Hydrothermal Activity Links Climate to
288 Tectonics: The Eocene Carbon Dioxide Greenhouse, *Science*, 227, 166-169.

289 Phipps Morgan, J., and B.K. Holtzman (2005), Vug waves: A mechanism for coupled
290 rock deformation and fluid migration, *Geochem. Geophys. Geosys.*, 6,
291 doi:10.1029/2004GC000818.

292 Resing, J.A., J.E. Lupton, R.A. Feely, and M.D. Lilley (2004), CO₂ and ³He in
293 hydrothermal plumes: implications for mid-ocean ridge CO₂ flux, *Earth Planet. Sci.*
294 *Lett.*, 226, 449-464.

295 Robock, A. (2000), Volcanic Eruptions and Climate, *Rev. Geophys.*, 38, 191-219.

296 Scheirer, D.S., K.C. Macdonald, D.W. Forsyth, S.P. Miller, D.J. Wright, M.H. Cormier,
297 and C.M. Weiland (1996), A map series of the Southern East Pacific Rise and its
298 flanks, 15 degrees S to 19 degrees S, *Mar. Geophys. Res.*, 18, 1-12.

299 Emter, D. (1997), Tidal triggering of earthquakes and volcanic events, in *Tidal*
300 *Phenomena*, edited by S. Bhattacharji et al., pp. 293– 309, Springer, New York.

301 Shackleton, N.J. (2000), The 100,000-Year Ice-Age Cycle Identified and Found to Lag
302 Temperature, Carbon Dioxide, and Orbital Eccentricity, *Science*, 289, 1897-1902.

303 Smith, D.K., M. Tolstoy, C.G. Fox, D.R. Bohnenstiehl, H. Matsumoto, and M. J. Fowler
304 (2002), Hydroacoustic Monitoring of Seismicity at the Slow Spreading Mid-Atlantic
305 Ridge, *Geophys. Res. Lett.*, 29, doi:10.1029/2001GL013912.

306 Stroup, D., D.R. Bohnenstiehl, M. Tolstoy, F. Waldhauser, and R.T. Weekly (2007), The
307 Pulse of the Seafloor: Tidal triggering of microearthquakes at 9°50'N East Pacific
308 Rise, *Geophys. Res. Lett.*, 34, doi:10.1029/2007GL030088.

309 Tolstoy, M., D.J. Fornari, and C.J. Fox (1999), Detailed Investigation of T-phase Swarms
310 on the East Pacific Rise, *EOS Trans. AGU*, 80, F1073.

311 Tolstoy, M., D.R. Bohnenstiehl, M. Edwards, and G. Kurras (2001), The seismic
312 character of volcanic activity at the ultra-slow spreading Gakkel Ridge, *Geology*, 29,
313 1139-1142.

314 Tolstoy, M., F.L. Vernon, J.A. Orcutt, and F.K. Wyatt (2002), Breathing of the seafloor:
315 Tidal correlations of seismicity at Axial volcano, *Geology*, 30, 503-506.

316 Tolstoy, M., J.P. Cowen, E.T. Baker, D.J. Fornari, K.H. Rubin, T.M. Shank, F.
317 Waldhauser, D.R. Bohnenstiehl, D.W. Forsyth, R.C. Holmes, B. Love, M.R. Perfit,
318 and R.T. Weekly (2006), A Seafloor Spreading Event Captured by Seismometers:
319 Forecasting and Characterizing an eruption, *Science*, DOI: 10.1126/science.1133950/.

320 Varadi, F., B. Runnegar, and M. Ghil (2003), Successive refinements in long-term
321 integrations of planetary orbits, *Astrophys. J.*, 592, 620-630.

322 Vogt, P.R., O.E. Avery, E.D. Schneider, C.N. Anderson, and D.R. Bracey (1969),
323 Discontinuities in Sea-floor Spreading, *Tectonophysics*, 8, pp 285-317.

324 Wilcock, W. S. D. (2001), Tidal triggering of micro earthquakes on the Juan de Fuca
325 Ridge, *Geophys. Res. Lett.*, 28, 3999-4002.

326

327 **Figure 1:** Mid-Ocean Ridge events confirmed to be magmatic/volcanic in origin through
328 observations of fresh seafloor lava and/or changes in vent fluid chemistry (see main text
329 for references). Event in grey on table (EPR 9N, 1991) was a confirmed eruption where
330 the timing is known well enough to categorize the month, but not well enough to
331 constraining fortnightly timing (Haymon et al., 1993). Red dots on the center plots
332 indicate timing of initiation of magmatic activity with respect to ocean tides (sea surface
333 height) [Matsumoto et al., 2000] at the location of the activity. Rose plot on the left
334 shows distribution of events with respect to phase of the fortnightly modulations of the
335 tides, based on the inflection points of an envelope function of the upper portion of the
336 tidal cycle. All but one of the events happen near the low in fortnightly tides, with four
337 happening just following the lowest point in the fortnightly modulations. Rose plot on the
338 right shows the distribution of events with respect to the month of the year (or orbital
339 eccentricity), with all events happening during the first six months of the year (increasing
340 distance from the sun).

341 **Figure 2:** Cartoon illustrating the concept of the response time of the system [Jupp et al.,
342 2004]. The load from the magma chamber is building through time (red line). For an
343 eruption to occur the "load function" must exceed the "strength function" (blue line) of
344 the overlying crust for a certain length of time ("response time"). When the load is near
345 the failure point, tidal stress will be pushing the load alternately above and below the
346 strength of the crust at diurnal and semi-diurnal intervals. However, if the response time

347 is greater than ~12-24 hours, the eruption would occur preferentially during the period of
348 subdued tides, when the load function is more likely to consistently exceed the strength
349 function for the required response time (days).

350 **Figure 3: (A)** Comparison of bathymetry from the Southern East Pacific Rise (SEPR)
351 (red line), CO₂ records from Antarctic ice-cores (blue line) [Lüthi et al., 2008, and
352 references therein], and orbital eccentricity (brown line) [Varadi et al., 2003]. Grey
353 vertical bars indicate periods of high orbital eccentricity. The bathymetry is an average of
354 nine ridge perpendicular lines on the western SEPR flank from 17°21'S to 17°29'S
355 (Supporting Figure S1) plotted versus age based on a half spreading rate of ~7.3 cm/yr
356 [Scheirer et al., 1996] (Supporting Text S2). The bathymetry profiles were demeaned and
357 filtered using a Butterworth high pass filter at 150 kyr to remove long-term lithospheric
358 cooling trends. Periods of low and high CO₂ appear to be roughly in phase with periods
359 of low and high crustal production, and low and high orbital eccentricity, particularly in
360 the most recent glacial cycles where timing is most accurate. As the age of the seafloor
361 increases, uncertainties in spreading rate compound, making timing of older bathymetric
362 variations less robust. **(B)** Normalized periodogram of Antarctic ice-core CO₂ (blue),
363 SEPR bathymetry (red) from (A), and eccentricity (brown) here also filtered at 150 kyr.
364 Seafloor bathymetry exhibits clear peaks at ~96 kyr, ~71 kyr and ~55 kyr, with much
365 smaller peaks at ~44 kyr and other higher frequencies. The CO₂ and eccentricity data
366 also show prominent peaks at ~95-96 kyr. CO₂ shows some deflection at ~71 kyr
367 relative to eccentricity and smaller peaks at higher frequencies. Eccentricity has a small
368 peak at ~55 kyr. Note that due to uncertainties in absolute spreading rate, including the

369 assumption of consistent spreading rate over this time scale, true timing of peaks may be
370 slightly different. Periodogram done using the Welch power spectral density method.

Figure 1

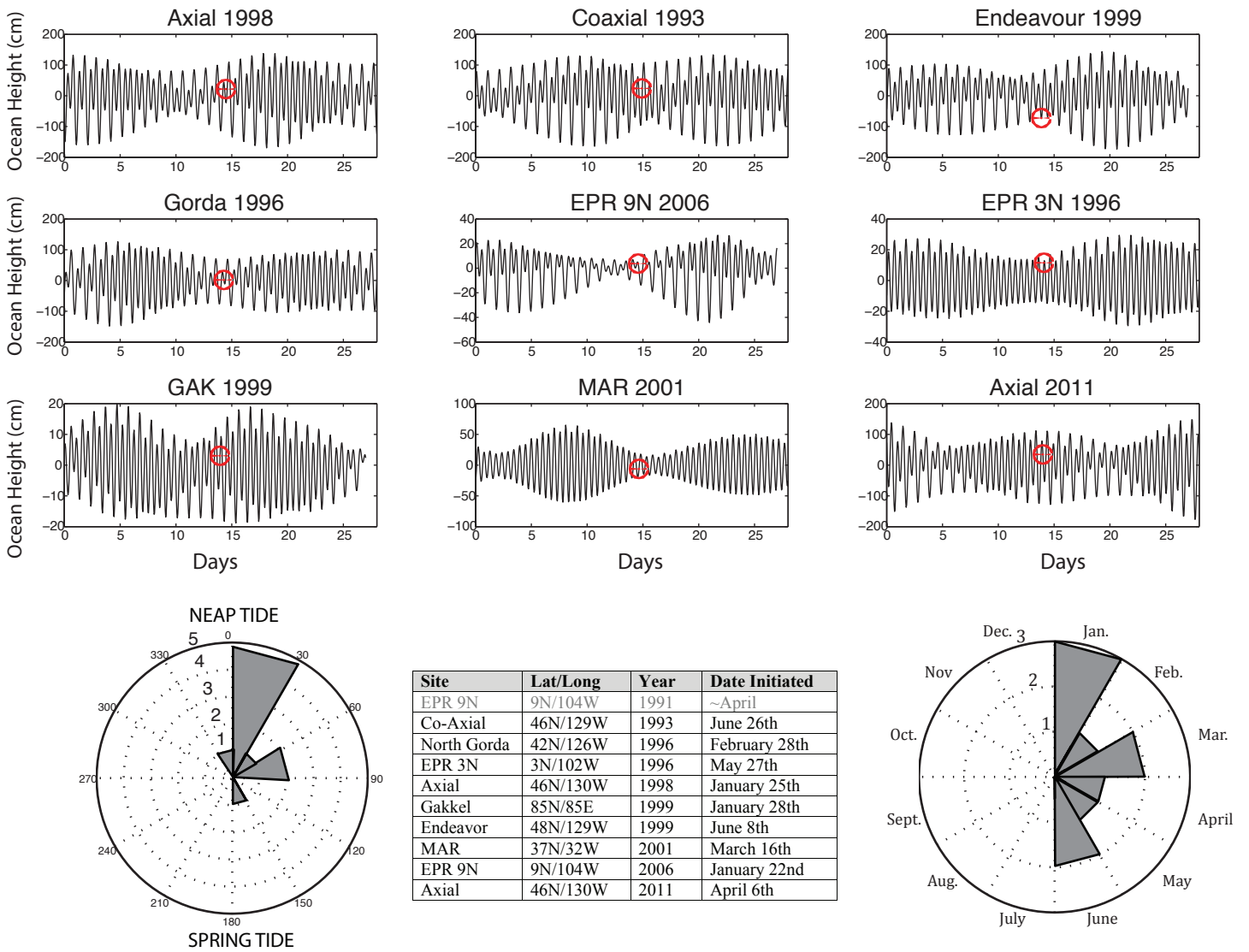


Figure 2

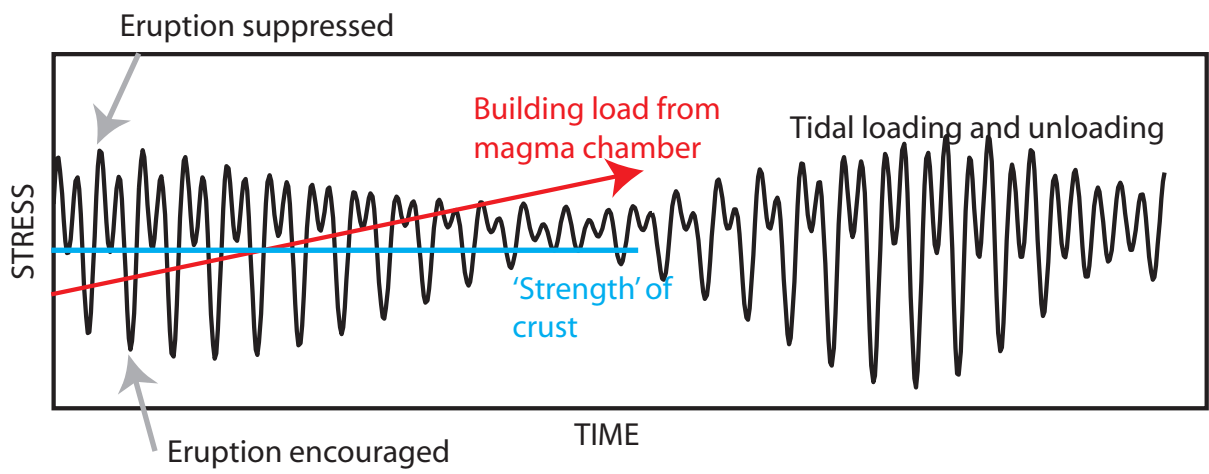
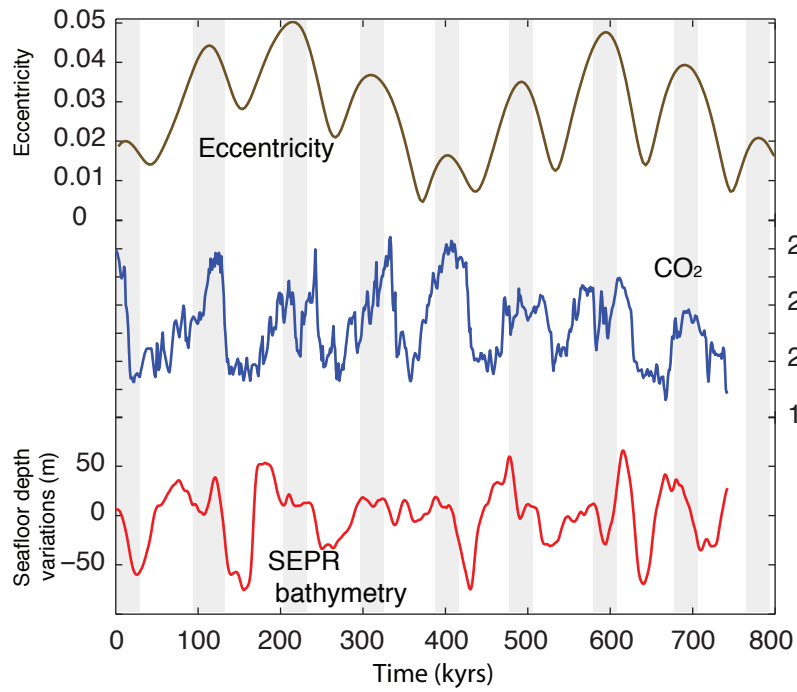
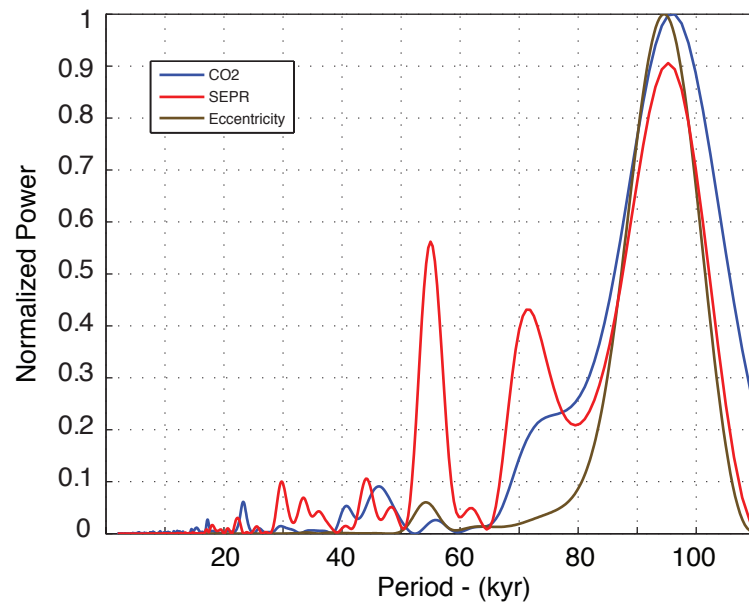


Figure 3



A



B